

AD-A135256

IRAAM
Wind Tunnel Test
Task III
Final Technical Report
Contract DAAK10-83-D-0009
AVSD-0343-83-RR

Prepared for
Department of the Army
U.S. Army Armament Munitions
and Chemical Command
Dover, New Jersey 07801

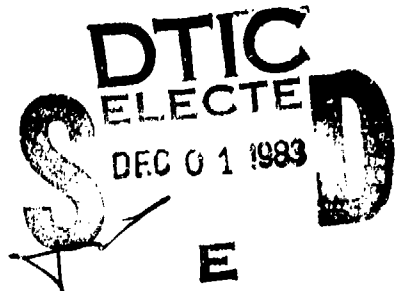
30 August 1983

Approved for Public Release;
Distribution Unlimited

Prepared by

Avco Corporation
Avco Systems Division
201 Lowell Street
Wilmington, Massachusetts 01887
(Middlesex County)

DTIC FILE COPY



83 12 01 008

IRAAM
Wind Tunnel Test
Task III
Final Technical Report
Contract DAAK10-83-D-0009
AVSD-0343-83-RR

Prepared for
Department of the Army
U.S. Army Armament Munitions
and Chemical Command
Dover, New Jersey 07801

30 August 1983

Approved for Public Release;
Distribution Unlimited

Prepared by
Avco Corporation
Avco Systems Division
201 Lowell Street
Wilmington, Massachusetts 01887
(Middlesex County)

Unclassified

SECURITY CLASSIFICATION OF THIS PAGE (When Data Entered)

REPORT DOCUMENTATION PAGE		READ INSTRUCTIONS BEFORE COMPLETING FORM
1. REPORT NUMBER	2. GOVT ACCESSION NO.	3. RECIPIENT'S CATALOG NUMBER
	AD-A135256	
4. TITLE (and Subtitle)	5. TYPE OF REPORT & PERIOD COVERED	
IRAAM Wind Tunnel Test Task III	Final Report	
7. AUTHOR(s)	6. PERFORMING ORG. REPORT NUMBER	
D. Dashcund	AVSD-0343-83-RR	
9. PERFORMING ORGANIZATION NAME AND ADDRESS	8. CONTRACT OR GRANT NUMBER (if)	
Avco Corporation Avco Systems Division 201 Lowell Street Wilmington, MA 01887	10-83-D-0004 DAAK-82-D-0009	
11. CONTROLLING OFFICE NAME AND ADDRESS	10. PROGRAM ELEMENT, PROJECT, TASK AREA & WORK UNIT NUMBERS	
	Delivery Order-0002 CDRL B0004	
14. MONITORING AGENCY NAME AND ADDRESS (if different from Controlling Office)	12. REPORT DATE	
	30 August 1983	
	13. NUMBER OF PAGES	
	15. SECURITY CLASS. (of this report)	
	Unclassified	
	15a. DECLASSIFICATION/DOWNGRADING SCHEDULE	
	N/A	
16. DISTRIBUTION STATEMENT (of this Report)		
Approved for public release; distribution unlimited		
17. DISTRIBUTION STATEMENT (of the abstract entered in Block 20, if different from Report)		
18. SUPPLEMENTARY NOTES		
19. KEY WORDS (Continue on reverse side if necessary and identify by block number)		
Skeet IRAAM Samara Blade Mine Vertical Wind Tunnel FASCAM		
20. ABSTRACT (Continue on reverse side if necessary and identify by block number)		
A deceleration, orientation and stabilization system for the deployment of the anti-armor mine (IRAAM) submunition was developed and tested at the Wright-Patterson vertical wind tunnel facility. The system employs a flexible samara airfoil with a tip mass arranged to provide the proper spin rate, descent rate and coning angle. → (over)		

DD FORM 1473 JAN 73 EDITION OF 1 NOV 65 IS OBSOLETE

SECURITY CLASSIFICATION OF THIS PAGE (When Data Entered)

Samara wings of KEVLAR material were fabricated using both a flat webbing construction and also a construction consisting of KEVLAR cords enclosed in a nylon envelope. Blades varied in both area and planform aspect ratio. Blade spans ranged from 2.5 to 10.0 inches. Blade widths varied from 2 to 4 inches.

All of the TRAAM models used for testing were dimensionally full scale. One model of the nominal configuration was full weight. The other two models were half weight. The tip weight varied up to 5% of the model weight.

The test program is outlined. All test procedures and equipment are described. The test results are analyzed and recommendations are made for future developmental studies.

Accession For	
NTIS GRA&I	<input checked="" type="checkbox"/>
DTIC TAB	<input type="checkbox"/>
Unannounced	<input type="checkbox"/>
Justification	
By	
Distribution/	
Availability Codes	
Dist	Avail and/or Special
A-1	



TABLE OF CONTENTS

	<u>Page No.</u>
Chapter 1: Introduction.	1
Section 1.1 Test Objectives	1
Section 1.2 Background.	3
Chapter 2: Test Articles.	5
Section 2.1 IRAAM Centerbodies.	5
Section 2.2 Samara Blades	7
Chapter 3: Spin Fixture and Wind Tunnel Facility.	14
Section 3.1 Spin Fixture.	14
Section 3.2 Wright-Patterson Vertical Wind Tunnel	16
Section 3.3 Instrumentation	18
Chapter 4: Pre-Tunnel Entry Testing	20
Section 4.1 Blade Integrity Tests	20
Section 4.2 Spin Fixture Tests.	21
Chapter 5: Test Observations.	23
Section 5.1 Setup	23
Section 5.2 Spin Fixture Launches	23
Section 5.3 Hand Launches	25
Section 5.4 Free-Flight Testing	26

TABLE OF CONTENTS (continued)

	<u>Page No.</u>
Chapter 6: Test Results	30
Chapter 7: Conclusions and Recommendations.	33
Section 7.1 Experimental Data	33
Section 7.2 Tunnel Facility	34
Section 7.3 Model Launch.	36
Section 7.4 Samara Blade Configurations	37

LIST OF FIGURES

	<u>Page No.</u>
Figure 1.0-1 IRAAM Samara Model	39
Figure 2.1-1 Photograph of IRAAM Samara Centerbody Models	40
Figure 2.1-2 Schematic Of IRAAM Samara Centerbody Models.	41
Figure 2.1-3 Photograph of IRAAM Samara Wind Tunnel Model Showing Component Assembly	42
Figure 2.2-1 Schematic of Webbing Type Blade Construction	43
Figure 2.2-2 Schematic of Corded Type Blade Construction.	44
Figure 3.1-1 Photograph of Spin Fixture in Wright-Patterson Vertical Wind Tunnel	45
Figure 3.1-2a Schematic of Crane Boom Moment	46
Figure 3.1-2b Schematic of Spin Fixture.	47
Figure 3.1-3 Photograph of Spin Fixture in Cocked Position with Saboted Model Inside	48
Figure 3.1-4 Photograph of Spin Fixture After Release of Model. . . .	49

LIST OF FIGURES (continued)

	<u>Page No.</u>
Figure 3.2-1 Schematic of Wright-Patterson Vertical Wind Tunnel.	50
Figure 5.2-1 Sketch of Typical IRAAM Samara Flight Behavior Following Launch Using the Spin Fixture.	51

LIST OF TABLES

	<u>Page No.</u>
Table 1.2-1 Samara Blade Parameters Tested.	52
Table 2.1-1 IRAAM Samara Centerbody Geometry and Mass Properties Wright-Patterson Vertical Wind Tunnel Tests of April 4-8, 1983.	53
Table 6.1-1 Test Data: Wright-Patterson Vertical Wind Tunnel Testing of IRAAM Samaras, April 4-8, 1983.	54

Chapter 1: Introduction

This report documents wind tunnel testing of the samara blade concept for the IRAAM program as conducted by AVCO in the Wright-Patterson Vertical Wind Tunnel Facility, WPAFB, Dayton, Ohio during the week of April 4-8, 1983. These tests were performed in support of the development of the samara blade as a submunition decelerator/stabilization and orientation device in the current XM898 (previously IRAAM) program. The samara blade concept, as conceived by Roy Kline of ARRADCOM/LCWSL/Applied Sciences Division, is that of a cloth fabric blade which when attached to a spinning body behaves like a single bladed rotor in poweroff, autorotative, descent. In doing so the samara blade decelerates the body and causes it to spin at a constant nondimensional spin rate given by the ratio of bladetip rotational speed to body axial velocity. Thus, a particular deceleration and coning motion can be imparted to the body. Figure 1.0-1 shows the model samara tested.

This work was performed under Contract No. DAAK-10-82-D-0009.

Section 1.1 Test Objectives

The general objective of the free-flight tunnel tests reported herein was to determine the performance characteristics of a IRAAM samara (i.e. a IRAAM submunition with a samara blade) in steady state, equilibrium, autorotative descent. In particular these tests were designed to experimentally determine

the samara blade configuration(s) which give the desired terminal sink (descent) rate, spin rate, and coning motion to the submunition. The desired coning motion of the body is constant lunar motion of the body at a fixed body tilt (or body coning) angle to the vertical (i.e. no nutation and/or precession with fixed body orientation with respect to the spin axis).

The specific objective was to test a 1:1 scale/mass model of the then current IRAAM submunition design to determine a samara blade configuration which gives the desired terminal flight deceleration and coning motion characteristics for proper submunition operation. At the time of testing the then current IRAAM submunition design had a height/diameter ratio of 3.6 inches/5 inches and a nominal weight of 8 lb_f. Also at the time of testing the desired steady state, equilibrium, autorotative, terminal flight conditions were:

sink rate:	100-120 f _{ps}
spin rate:	30-40 Hz
body tilt angle:	25-35 deg

In addition, the blade designs tested were to be packageable and of sufficient structural integrity to withstand fullup deployment loads.

The vertical wind tunnel tests consist of the following: The IRAAM samara models were right circular cylinder centerbodies with attached cloth fabric samara blades. The outboard end of the blade held a bladetip airfoil/weight. The models were launched into the tunnel flow at low spin rates either by hand or with a spin fixture. As the model spun up in the flow, the tunnel operator attempted to keep the model within the vertical extent of the tunnel test section by controlling tunnel airspeed. Once the free-flight model achieved

steady state, equilibrium, autorotative flight, it was vertically positioned at camera level by careful control of tunnel airspeed. A high speed movie camera was used to record the flight of the model from launch. The airspeed at which steady state autorotation occurred was recorded. The equilibrium spin rates and body tilt angles were measured off the developed film. In addition, qualitative assessments of flight stability, precessional/nutational motion, and any tendency toward translatory motion were made.

Section 1.2 Background

AVCO has previously free-flight tested IRAAM/samara blade designs in the Langley spin tunnel facility. Due to a tunnel airspeed limit of 80 fps and safety related restrictions on the blade tip mass and spin rate, a twice geometric scale, quarter weight samara model was flown in the Langley tunnel. The model had a height/diameter ratio of 7.2 inches/10 inches and nominally weighed 2 lb_f.

Two tunnel entries were made, one in December 1981 and the other in June 1982. For the first entry, the blades were mounted on the side of the IRAAM centerbody at one of three axial locations. Blade root incidence was varied between 20 and 50 degrees nose down to the horizontal. In addition the effects of blade sweep and blade tip camber were also investigated. The second Langley entry examined mounting the blades off the top of the IRAAM centerbody, in as much as this appeared to be a more advantageous arrangement for blade packaging. For this series of tests, blade sweep and root incidence variations were eliminated. The principal blade parameters varied were blade

span, from 0.5 to 1.5 cal, and blade root location from the model center (from .2 to .5 cal). The specific blade configuration parameters tested are given in Table 1.2-1 for both tunnel entries.

At Langley, configurations which flew stably could be flown in steady state flight essentially indefinitely. The tunnel operator was able to hold the spinning/coning IRAAM sarara models at a fixed level in the tunnel for a time interval of sufficient length to ensure steady state conditions had been achieved and to permit the acquisition of good film data.

Chapter 2: Test Articles

Section 2.1 IRAAM Centerbodies

The IRAAM centerbodies tested were right circular cylinders. Three geometrically full scale centerbodies were tested, two with a height/diameter ratio of 3.6 inches/5 inches and the third with a ratio of 4.32 inches/5 inches. These height/diameter ratios correspond to packaging six or five IRAAM's, respectively, in the M483A1-155 mm carrier round. A photograph of the IRAAM centerbody models tested is given in Figure 2.1-1.

The two 3.6/5 height/diameter ratio centerbodies nominally weighed 4 and 8 lb_f . The payload capability of the carrier round is nominally 48 lb_f ; so, these 4 and 8 lb_f IRAAM models correspond to half and full weight models, respectively, of the six per carrier round submunition. The 4.32/5 height/diameter ratio centerbody nominally weighs 4.8 lb_f corresponding to a half weight model of the five per carrier round submunition. The actual weights of the centerbodies tested were slightly lower than these nominal values to accommodate blade and blade tip weights up to 5 percent of total IRAAM samara model weight. The centerbody models were constructed to duplicate c.g. locations and the axial and transverse moments of inertia of the then current IRAAM submunition designs. The c.g. locations were slightly below center for all three centerbody models and the ratios of axial to transverse moments of inertia about the c.g. were approximately 0.75 for the 3.6/5 centerbodies and 0.85 for the 4.32/5 centerbody. The products of

inertia were nominally zero for all three IRAAM samara centerbody models. Table 2.1-1 summarizes the basic geometry and specific mass properties of the IRAAM centerbodies tested.

A schematic of the IRAAM centerbody model construction is given in Figure 2.1-2. The half weight models consisted of an outer steel sleeve with an inner Lexan core. The full weight model was constructed with a steel sleeve and an aluminum core. The cores were press fitted into the sleeves and held there using four screws. The base of the core, opposite the blade attachment end, was flush with the base of the sleeve. As such the centerbody models with their flat bases did not model the concave geometry of the warhead liner nor the external envelope of a possible MMW antenna mounted on the base. The tops of the cores were recessed approximately 0.4 inches below the top of the sleeves to leave space for packaging the blade and blade tip weight. The top of each core had two cutouts with hold-downs to permit attachment of the blade at four different locations: one along the curved inside surface of the sleeve (referred to as the curved blade root constraint) and the other straight blade root constraints at three different radial distances from the centerbody center. The bottom longitudinal edges of the blade hold-downs were grooved to accommodate the blade root end wrapped around an aluminum pin and sewn. Only blade root attachments on top of the centerbody were considered in these wind tunnel tests. Figure 2.1-3 shows a disassembled IRAAM samara model with the two blade hold-downs removed and two representative samara blades.

Section 2.2 Samara Blades

The samara blades were constructed using cloth materials; they are therefore non-rigid, flexible blades. All blade configurations tested had constant chord, rectangular platforms. Two different blade design types were fabricated: one type using Kevlar (para-aramid) webbing and the other using Kevlar braided cords sewn to a nylon backing material. The two different blade types permitted mounting the blade either along the curved inside surface of the sleeve or straight across the top of the centerbody without a tendency for the blade to pucker under a chordwise uniform tensile load. That is, both blade types were designed to lie flat under a uniform chordwise tensile load such that a uniform load at the blade tip produces uniform loading along the chordwise length of either the curved or straight root constraints. Blades of both types with three different chord lengths (2, 3, and 4 inches) and four different spans (2.5, 5.0, 7.5, and 10.0 inches) were fabricated.

Webbing Blades

Figure 2.2-1 gives a schematic of the webbing type blade fabrication details. The webbing blades were constructed using individual plies of 1 and 2 inch width Kevlar ribbons rated at 1000 and 2000 lb_f tensile strength, respectively. As shown the single ply of material was folded back on itself at the outboard blade tip end and sewn to form a pocket for the blade tip

airfoil/weight. At the blade root both plies form a sewn loop for the blade root constraint pin. The two plies were stitched together along the blade leading and trailing edges and X's were also stitched across the blades to keep the plies together. Figure 2.1-3 shows, in the foreground, a representative straight webbing type blade. Shown with the blade is a blade root hold down with grooved bottom edges designed to accept the pinned blade roots. The blade spans were measured from the blade tip to the top of the model cores. An additional 1.3 inches of span to the center of the blade root pin loop were required for blade root attachment.

As constructed the 2 inch chord blades have a nominal tensile strength of 4000 lb_f with proportionately higher tensile strengths for the wider chord blades. The highest blade tip centrifugal load expected was approximately 800 lb_f. This corresponds to the largest blade tip weight of 0.4 lb_f (5 percent of the 8 lb_f, full weight model) and the largest blade radius, nominally 12.5 inches (10 inch blade span mounted on the centerbody's cylindrical edge), spinning at a maximum spin rate of 40 Hz. The anticipated centrifugal loads are proportionately less for the lighter tip weights and shorter blade radii. Thus all the blades fabricated had a minimum safety factor of 5 to accommodate any chordwise non-uniformity in the centrifugal load due to non-uniform blade tip mass distribution. In addition the higher than necessary tensile strength blade design is more representative of the blade construction characteristics required to withstand deployment at spin rates up to 170 Hz for the actual submunition.

Blade Tip Pocket

The blade tip pocket loop was sized to hold a blade tip airfoil/weight with up to a 1 in² cross section area. A piece of Kevlar tape was sewn into the leading edge of the pocket loop to restrain the forward movement of the tip weight. A flap of Kevlar material was added to the pocket loop's trailing edge so that during wind tunnel testing the blade tip airfoil/weight could be changed, the flap of material tucked into the pocket around the top airfoil's trailing edge, and the pocket trailing edge sewn closed by hand. Use of a blade tip pocket design with high tensile and ballistic penetration strength ensured retention of the blade tip weight while permitting use of the same blades with several different blade tip weights for both the half and full weight models. Use of a sealed Kevlar pocket to attach the blade tip weight to the blade also ensures that in the event the blade tip strikes the tunnel periphery and a portion of the tip airfoil plate/weight assembly shears, the fragments thereof would be contained within the pocket.

The limitations of the blade tip pocket design include: The blade pockets were sized to accommodate a blade tip weight with a cross section of 1 in² corresponding to the largest tip weights to be tested at the most forward c.g. chord location for the shortest chord blades. For smaller, lighter tip weights the excess, unfilled pocket material results in a slightly increased blade span. The shape of the blade tip pocket leading edge closure is aerodynamically not clean resulting in high blade tip drag. In general the variability of the blade tip pocket geometry under centrifugal and aerodynamic load for different blade tip weights results in variable and irregular blade

tip aerodynamic performance. The difficulty is in determining whether variations in IRAAM samara performance with changes in blade tip airfoil weight are due to changes in the weight itself, including its effect on blade lofting (aeroelastic cambering), or to its effect on the blade tip geometry. Additionally any variation could simply reflect the uncontrolled, irregular nature of the cloth pocket geometry as constructed.

Corded Blades

The cord type blades were designed for attachment to the IRAAM centerbody along the curved inside surface of the outer sleeve. Use of the corded construction permits the blade under chordwise uniform tensile load to remain flat to the edge of the sleeve and then transition to the sleeve's curved inside surface, transmitting a uniform tensile load along the length of the curved root constraint. Whereas if a webbing type blade is constrained at the root to the inside curved surface of the sleeve, a uniform tensile load at the blade tip unequally loads the blade root such that the leading and trailing edges carry more tensile load than does the center of the blade. As a result, under aerodynamic load the inboard section of the blade is freer to loft (i.e., aeroelastically camber) and thereby alter the blade section aerodynamics. For the corded blades the blade angle at which the plane of the untwisted blade intersects a plane normal to the cylindrical surface of the sleeve was set at 30 degrees (see Figure 2.2-2). Since the blade coning angle is typically near zero, i.e. the blade flies in the horizontal plane, and since the design centerbody tilt angle (or centerbody coning angle) as

measured between the axis of the centerbody and vertical is 30 degrees then the desired blade angle with respect to the centerbody (as described above) is also 30 degrees. Therefore the cord type blades were fabricated with a "built-in" blade angle of 30 degrees.

Figure 2.2-2 schematically shows fabrication details for the corded blades. The Kevlar braided cords were sewn to one side of a nylon backing material which was hot knifed to the correct blade chord dimensions. In a way identical to that used for the webbing blades, the corded blade material was folded back on itself, cords on the inside, to form a blade tip pocket loop. The pocket area was reinforced by securing a piece of Kevlar to the inside of the pocket loop. Otherwise the details of blade tip pocket construction and the associated limitations of this blade tip airfoil/weight attachment method are the same as previously given for the webbing blades. Eight 300 lb_f tensile strength braided Kevlar cords were straight stitched to a nylon canopy cloth backing material. Eight such cords equally spaced across the chord of the material were used for all three blade chord widths of 2, 3, and 4 inches. With this corded material folded back on itself there are sixteen cord cross sections per blade cross section; therefore, the nominal tensile strength of the corded blades was 4800 lb_f.

Along the curved edge where the plane of the blade intersects the cylindrical inside surface of the sleeve, the inboard ends of the blade backing material were cut to match this curved edge. The curved ends of the two plies were butt sewn to straight edged pieces of backing material which make up the blade root portion of the blade. The cords are sewn down onto

these sections and both ends were wrapped to form a loop for the pin and sewn. In transitioning from the nominally flat blade surface to the curved surface of the sleeve the overall cord lengths toward the center of the blade are therefore progressively shorter than those at the leading and trailing edges. Figure 2.1-2 includes a representative cord type blade with its blade tip pocket open and a representative blade tip airfoil plate and weight resting on the trailing edge flap of the pocket. The root portion of the blade has been propped up to show how it conforms to the curved surface of the adjacent hold-down. A curved pin restrains the root of the blade in the curved bottom groove of the hold-down.

Blade Tip Weight

The nominal shape of the blade tip was previously given in the description of overall blade fabrication. As discussed earlier, the shape of the blade tip airfoil pocket and therefore its aerodynamic characteristics are variable and irregular depending on, among other things, the aerodynamic and centrifugal loading as well as the dimensions of the blade tip weight. As shown in Figure 2.1-3 the blade tip weight consisted of an aluminum plate with a lead weight bolted to the plate. The aluminum plates were 1/16 inch thick with a 1 inch span and a 2, 3, or 4 inch chord to match the blade chord. Two slots were cut in the forward half of each plate to accept a bolted on lead weight whose chordwise c.g. position could be varied anywhere from 10 to 50 percent behind the leading. Lead weights were fabricated to permit

incremental variation of the overall blade tip weight. The blade tip weights made were nominally 0.4, 0.3, 0.2, and 0.1 lb_f and half these values corresponding to 5, 3.75, 2.5, and 1.25 percent of the total model weights of the full and half weight 3.6/5 height/diameter IRAAM models.

Chapter 3: Spin Fixture and Wind Tunnel Facility

Section 3.1 Spin Fixture

A spin fixture was designed and fabricated to spin up and launch the IRAAM samara models into the tunnel flow. Figure 3.1-1 shows a photograph of the spin fixture arrangement in the tunnel. As shown, the spin fixture was mounted on the end of a 10 ft. section of aluminum channel pivoted off the bottom of the existing traveling crane boom. The crane boom was positioned just within and tangent to the throat of the tunnel. The pivot point therefore was just on the edge of the test section and the 6 ft length of the spin fixture from the pivot permitted it to be rotated into the center of the tunnel flow for launch. The channel/crane boom attachment is shown schematically in Figure 3.1-2. It was intended that the channel would be supported off the top of the crane boom; but due to limited clearance between the top of the boom and the lower edge of the diffuser bell, the channel attachment was improvised and the channel mounted on the underside of the boom.

Also shown in Figure 3.1-2 is a schematic representation of the spin fixture. The spin fixture consists of an aluminum spin can bolted onto a short shaft which was press fitted into a set of ball bearing housings mounted on the channel. The inner races of the bearings were also set screwed to the shaft. The spin can was belt driven using a variable speed controlled AC motor. The IRAAM samara model fits inside a nylon sabot which in turn fits inside the spin can. The sabot model was held in place inside the spin can

during spin up by an external, spring loaded support/release bracket as shown. The base of the sabot model in the spin can rides on a single, large ball bearing mounted on the horizontal member of the bracket. The bracket is held in place by a pin which when pulled releases the bracket which swings clear of the bottom of the model leaving it free to drop into the tunnel flow. Figure 3.1-3 shows a photograph of the spin fixture with the support/release bracket cocked holding the sabot model in the spin can. Figure 3.1-4 shows a photograph of the spin fixture after release of the model. This figure also shows the arrangement for mounting the spin fixture channel off the crane boom.

The sabot was used to ensure that the samara blade did not deploy until the model had fallen clear of the spin fixture. Torque is transmitted from the spin can to the sabot using two vertical pins in the bottom of the spin can and corresponding holes in the top of the sabot. The torque is in turn transmitted to the IRAAM samara model by two horizontal pins in the side of the centerbody which match two holes in the sides of the sabot. On model release these pins pull the sabot out of the spin can with the model. Sufficient head height, approximately 1 inch, between the top inside surface of the sabot and the top of the model centerbody core was provided to accommodate those blade tip weights with the greatest thickness. The blades were accordion folded within the recessed top of the model centerbodies with the blade tip positioned radially up against the inside edge of the sleeve tip. The two halves of the sabot are then positioned over the top of the centerbody and the assembly is then ready to be loaded into the spin fixture. In general the blade and blade tip airfoil/weight were not otherwise restrained prior to deployment nor was any means attempted to control the actual blade deployment.

Section 3.2 Wright-Patterson Vertical Wind Tunnel Facility

The Wright-Patterson Vertical Wind Tunnel facility is shown schematically in Figure 3.2-1. The open throat test section has a diameter of 12 ft. and an approximate height of 12 ft. from the bottom lip of the test section to the bottom lip of the diffuser bell. A horizontal safety net was positioned just below the bottom lip of the test section. The interior of the diffuser bell extends the free flight test area above the test section by approximately 12 ft. to the nose of the bullet shaped housing below the propellar hub or 16 ft. to the metal grating just below the propeller. A vertical net was also installed around the open test section to contain the free flight models. As previously shown in Figure 3.1-1 the crane boom was positioned so that the spin fixture channel pivot was just inside the vertical net. With the spin fixture pivoted into the center of the tunnel, its height above the bottom horizontal safety net was approximately 13 ft.

The tunnel airflow is driven by a 16 ft. diameter controllable pitch fan with laminated maple blades. The fan is driven by a 1000 hp DC motor with a Ward Leonard speed control system. The maximum tunnel airspeed is approximately 150 fps without the lower safety net present and 135 fps with the net. Available pitot tube rake survey data shows the velocity profile of the tunnel flow to be flat, within ± 2 fps, from the center of the tunnel to within a foot of the throat periphery. The surveys were made at heights between 2 and 8 ft. above the lower lip of the test section without the horizontal safety net and vertical net in place. These results were obtained for tunnel airspeeds between 65 and 150 fps. Turbulence measurements with and

without the horizontal net in place showed turbulent velocity levels to be less than 2 percent of the mean tunnel velocity. The vertical net was not in place for these turbulence measurements. The airflow stagnation temperature and pressure are approximately ambient atmospheric.

As shown in the schematic, the tunnel operator sits behind the control panel outside the test section chamber. His position is approximately 8 ft. back from the lip of the test section throat behind a plate glass window. A camera operator with a high speed camera was positioned behind a second window 90° around from the operator. The camera operator's view is that of the test section with tunnel airspeed displayed digitally in the background at one location on the back wall of the test chamber. Plexiglass panels were installed in front of both plate glass windows to protect them and those test personnel behind them in the event part of a free flight model separates and is not contained by the vertical net.

Section 3.3 Instrumentation

The free flight tests of the IRAAM samara models were recorded on film using a 16mm high speed movie camera. All the film was shot at 200 frames per second. As previously stated, the principal objective of this series of wind tunnel tests was to establish the steady state, autorotative, flight characteristics of the various IR/AM samara configurations tested. This includes, as the primary goal, quantitative determination of steady state sink rate, spin rate, and centerbody coning (or body tilt) angle. The film record provided this information. The developed film was viewed on a Vanguard motion analyzer to determine spin rate and centerbody tilt angle. A clock time was digitally incoded on one edge of the film providing as absolute time reference. The tunnel airspeed was recorded on film as digitally displayed on a light board on the back wall of the test section chamber opposite the camera position. Just prior to launch the camera view included the airspeed display. Subsequent to launch, as the tunnel operator varies the tunnel airspeed in an attempt to keep the model within the vertical extent of the test section, the tunnel airspeed was only recorded when the plane of view of the camera tracking the free flight model happens to include the airspeed display. As will be discussed later, this is not a serious limitation when steady state flights of long duration are readily achievable. Under these circumstances, once steady state flight is achieved, the operator is able to vertically position the model in the test section to include the airspeed display, by small changes in tunnel airspeed. Indeed if steady state flight

of reasonable duration is achieved one can readily record the displayed airspeed by hand. In addition to obtaining these quantitative measurements, the film coverage was also intended to permit qualitative assessment of IRAAM samara flight stability; the transient behavior of the model following launch and in response to tunnel airspeed changes; any precessional, nutational motion of the spin axis; and any translatory motion of the samara in the horizontal plane. The high speed films were the only means used for data acquisition in these tests.

Chapter 4: Pre-Tunnel Entry Testing

Prior to tunnel entry, at the direction of Wright-Patterson Vertical Wind Tunnel test personnel, two tests were performed. One test addressed the structural integrity of the fabricated samara blades. The other test was a preliminary function check of the spin fixture and its release mechanism.

Section 4.1 Blade Integrity Test

Blade structural integrity tests were performed on two sample samara blades. A blade of each design type (webbing and corded) was tested. The two blades both had 3 inch chords and 10 inch spans. A 0.4 lb_m tip weight with a 25 percent chord c.g. location was sewn into each blade tip pocket. The two blades were mounted opposite to each other on the spin table to balance the centrifugal loads on the spin shaft. The radius of the blade tips from the spin axis was 10.75 inches. The design blade root pins restrained the blade roots. The blades were successfully spun up to a maximum spin rate of 25 Hz corresponding to a maximum centrifugal tensile load of 275 lb_f. It had been intended to test the blades up to a spin rate of 56 Hz corresponding to a factor of 2 beyond the highest spin rate of interest of 40 Hz and therefore a factor of 2 beyond design centrifugal loads; however a spin table with these higher spin rate capabilities was not available for these last minute tests. We therefore decided to restrict our wind tunnel testing to combinations of

blade span, blade tip weight, and spin rate which kept us below the tested centrifugal load. It should be noted, as previously mentioned, that the blade designs were structurally very conservative, with safety factors of at least 5 over the design loads.

Section 4.2 Spin Fixture Tests

Prior to tunnel entry the spin fixture was tested to ensure that it would spin up and release the IRAAM samara models. The tests were conducted in an enclosed area allowing a 2 ft drop between the spin can and the padded bottom of the enclosure. The spin fixture was mounted on its channel and supported in such a way as to roughly approximate the wind tunnel set up in order to check for adverse structural resonances during spin up. High speed movie camera coverage was used to record and document the tests. Tests were conducted using the full weight IRAAM model with a 3 inch chord; 10 inch span, 0.4 lb_m tip weight samara blade. It was intended that the full weight model be launched at spin rates up to 40 Hz. Testing showed that the maximum spin rate at which the sabot model would release from the spin fixture was 15 Hz. Evidently the friction due to centrifugal loads acting on the two halves of the clamshell sabot prevented the model from dropping clear at higher spin rates. As an alternative, vertical slots were added to the sides of the sabot which let the model drop free leaving the sabots behind in the spin can. Using this arrangement the model would release at spin rates up to 20 Hz. Except for this limitation the spin fixture/release mechanism functioned smoothly and

it was judged adequate for the proposed wind tunnel tests. Previous wind tunnel testing of similar configurations by Walter Koenig of the ARRADCOM/LCWSL/Applied Sciences Division had demonstrated successful hand launches at lower spin rates than those achievable using the spin fixture. During these spin fixture tests the blade deployed readily though there was a tendency for the blade to twist up on itself.

Chapter 5: Test Observations

Section 5.1 Setup

Placement of the crane boom and the spin fixture channel pivot point just within the vertical net required an improvised extension of the vertical netting about the boom and channel to ensure that the free flight models would be contained within the tunnel test section. In addition, for safety reasons during initial testing, the spin fixture was setup for remote operation of the spin motor speed control and model release from outside the test section chamber.

Section 5.2 Spin Fixture Launches

Initial testing used the spin fixture to launch the models. Launches were made both with and without the model sabot. As in earlier pre-tunnel entry testing, if the spin rate was kept low enough the sabot model readily dropped out of the spin can upon release of the support bracket. In those instances when the model did hang up in the spin can the spin rate was reduced to the point where the model did drop. In all instances once the model cleared the spin can the clamshell sabot cleanly separated initiating blade deployment.

Subsequent to launch the following sequence of events was typically observed (see Figure 5.2.1). Initially, during blade deployment, the tendency was for the blade to twist up as the centerbody continued to spin

beneath the deploying blade. It appeared that the blade, as deployment begins, initially stalls and pitches nose down slowing the blade's circumferential component of motion as the centerbody continues to spin, twisting the blade one or more wraps. At blade stretch, when the twisted blade had fully deployed, it would pull the centerbody on its side (body tilt angle approximately 90 degrees to the vertical) as shown. The blade would then typically untwist itself, pitching nose up, until it was essentially flat and fully deployed flying trailing edge forward with the centerbody still pulled over on its side. Then with the blade still flying backwards overhead the centerbody would right itself into a nearly flat spin (body tilt angle approximately 0 degrees). Finally the blade overhead would pitch leading edge up as the spinning centerbody pulls the blade around causing the blade to straighten out into its normal flight orientation. Though typical of most spin fixture launches, in most instances this "blade recovery" was incomplete before the model had dropped to the bottom safety net ending the flight. There were, however, several instances in which full recovery did occur above the bottom net and the flights continued.

An almost identical initial flight behavior was observed for those launches made without the sabot. The only significant difference was in the way this characteristic motion was initiated. As anticipated, in launches without the sabot the blade tip weight tended to "hang up" on the inside surface of the spin can, held there by the centrifugal load, as the centerbody dropped away from the can. In those instances when it did hang up the blade tip would eventually work itself clear as the spin fixture despun reducing the centrifugal force on causing the blade to twist up and thus free itself from

the can. Several ways of taping down the blade tip were tried in an attempt to prevent early deployment of the bladetip inside the spin can. These improvised attempts to delay blade deployment were only marginally successful. In either case the blade tip's rotational component of motion was initially slowed compared to that of its root resulting in the blade twisting and subsequent flight behavior as described above.

As a whole, therefore, the flight behavior of the IRAAM samara following spin fixture launch was reasonably "forgiving" in that it appeared that in most cases had there been enough vertical drop available the blades would have recovered and the flights could have continued. No tendency was observed for significant lateral, translatory motion of the samara following blade stretch. The initial flight paths were essentially vertical from release. It should be remarked that spin fixture designs in which the samara is spun up and launched with the blade already deployed were considered and judged to give more promise of successful model launch. However design complexity as well as time, effort, and cost considerations precluded pursuit of this alternative spin fixture design concept. Due to the difficulties encountered using the spin fixture, the majority of flights were launched by hand.

Section 5.3 Hand Launches

Hand launching was considered as a viable alternative to use of the spin fixture based on previous experience with free flight samara testing at the Langley spin tunnel as well as observation of ARRADCOM's own testing of samara at Wright-Patterson. The advantage of hand launching is that it permits

launches with the blade deployed. The disadvantage is that hand launch requires a certain amount of experience and skill to achieve successful launches with any regularity. The major problem encountered was one of imparting too much translational motion to the model during launch causing it to immediately translate into the side vertical nets. In addition it is not particularly easy to hand spin the model fast enough or flat enough for successful launch. Experience showed we were successful perhaps one out of five tries at successfully hand launching a model. In addition, there are increased safety concerns associated with hand launching.

Section 5.4 Free-Flight Testing

Following successful launch of the model samara, the test procedure is to fly the model long enough, by controlling tunnel airspeed, for it to achieve steady state, equilibrium, autorotative flight. Having achieved steady state autorotation, careful control of the tunnel airspeed permits vertical positioning of the free-flying model at a height in the test section the same as that of the camera. This permits a film record to be made from which one can readily measure centerbody tilt angle in addition to steady state spin rate. If steady state autorotation of sufficient duration is achieved there is no difficulty in establishing and recording what the tunnel airspeed is, corresponding to steady state sink (descent) rate.

The testing at Wright-Patterson showed that, assuming one managed to successfully launch a IRAAM samara model, whether by hand or using the spin

fixture, it was very difficult to fly it long enough to obtain and be sure that one had obtained steady state, equilibrium, autorotative flight. Typical flight times following successful launch were on the order of 5 to 10 seconds in duration. For most configurations the flight behavior appeared stable, as if steady state flight was possible. However, in most cases the models were not kept flying long enough to clearly establish steady state flight conditions. Typically the models were still in transient flight, still spinning up and still climbing and descending in response to the tunnel operator's attempts to hold the model fixed in the flow when the flights ended.

Most of the flights ended as a result of the model translating laterally into the vertical net or the sidewall of the diffuser bell. Either the blade tip would snag in the netting or come to an abrupt halt on impacting the diffuser wall. Previous test experience in the Langley spin tunnel showed that with its relatively pronounced dish shaped velocity profile the higher velocities near the sidewall tended to keep the model away from the walls. The higher velocities near the wall increase the thrust on the wall side of the samara rotor tilting its net thrust vector away from the wall. This change in thrust direction slows the lateral translational motion of the model preventing it from hitting the wall or slowing it sufficiently so that the blade tip just glances off the test section walls. As previously mentioned, the velocity profile in the Wright-Patterson tunnel is essentially flat, therefore there is no tendency for the model to remain near the center of the tunnel flow. In an attempt to modify the velocity profile by creating a velocity depression in the center of the flow an 8 in. diameter 1/2 inch square mesh screen was installed on top of the honeycomb flow straightener at

the intake to the convergent section leading into the test section. Measurements made following the samara wind tunnel tests showed that the velocity in the center of the flow was reduced to 86 percent of that indicated in the flow periphery. All but the first configurations were tested with the screen installed. This modification did appear to help a little, but not as much as one would have liked. The details of the modified velocity profile generated are not known. Possibly the high velocity area near the periphery of the flow was too abrupt or too brief in radial extent to slow the translational motion of the models. The combination of open throat test section and vertical net prevents flight recovery when the outward radial motion of the model is not completely stopped before the blade snags the net. In addition the net's effect on the velocity profile with or without the screen installed is unknown. Also, any radial component of tunnel flow due to the fact that the tunnel is open throated would also tend to drive the free-flying models radially outward. It should be noted that for most of the testing, personnel were positioned around the lip of the tunnel throat with 2 ft. by 3 ft. pieces of plywood which were used to deflect the tunnel flow near the periphery in an attempt to redirect the translating model and keep it flying in the tunnel flow. This is a relatively standard lateral model control method used in the Wright-Patterson facility. With experience this procedure was somewhat effective though it was difficult to cover all quadrants of the tunnel at all heights. In addition there are safety concerns associated with this practice.

Another major difficulty is that the tunnel operator's field of view from his position behind the control console outside the test section chamber is

limited essentially to the test section itself. The operator can only see a small portion of the test space inside the diffuser bell. Thus, if the model flies up beyond the diffuser bell lip the operator can no longer track the model and there is little hope of the flight continuing. In many instances the models leveled off near the top of the tunnel, but because they were beyond the operator's view he continued to slow the tunnel flow too much and too fast to permit recovery when the model dropped back into his view.

Other difficulties associated with this type of testing are as follows: Attempting to hold the free-flight model vertically fixed in the flow requires fast response by the operator to changes in the model's position in the tunnel, as well as fast response of the tunnel flow in response to the operator's throttle inputs. It is not clear in the case of the Wright-Patterson facility whether the tunnel operator has sufficient command authority to change the flow velocity rapidly enough. There may be too great a lag in flow response to throttle input which cannot be adequately anticipated and overcome by the operator. Based on previous experience free-flying samara in the tunnel the operator's throttle control had been modified in an attempt to improve the control response time and authority. There may have been some improvement; it is difficult to assess. It perhaps should be noted that experience flying free-flight models in the tunnel contributes significantly to the operator's capability to successfully control the model. While the Langley facility has been used extensively over many years for free-flight spin testing, the Wright-Patterson facility has only recently been reopened and there is not the same amount of experience in conducting such experiments.

Chapter 6: Test Results

Of the 36 IRAAM samara configurations tested only 27 of them were launched successfully, after repeated tries, and had long enough flight times to obtain useful data from the film record. As discussed in the previous chapter, most of those configurations which were observed to be relatively stable never achieved steady state, equilibrium, autorotative flight or at best achieved it only momentarily before the flight abruptly ended. Nevertheless, for all 27 configurations for which flight measurements could be made, a best value assessment of steady state or near steady state flight conditions was made. Therefore for each configuration values for terminal sink rate, spin rate, and body tilt angle were determined as best as they could be determined. In general, therefore, the data is somewhat suspect and should be used with care in trying to assess the terminal flight performance characteristics of the IRAAM samara tested.

Probably the best two flights conducted in terms of flight duration and closest approach to steady state flight were the two flights listed for the full weight, 3.6/5 height/diameter ratio IRAAM samara. These are experimental flights numbered 33 and 36. Their steady state sink rates and spin rates were within the then current design sink and spin rates of 100-120 fps and 30-40 Hz. However, body tilt angles obtained using blade tip weights that were nominally 1.25 and 2.5 percent of total model weight were lower than the desired design value of 30 degrees. The flight sequences 3-4-6 and 14-16-18 in which only the blade tip weight was varied from 5 to 1.25 percent of

total model weight clearly show a direct correlation between bladetip weight and body tilt angle. Increasing blade tip mass increases body tilt angle. If indeed body tilt angle is primarily a function of the inertial properties of the IRAAM samara, specifically the tilt of the centerbody's principal axis of rotation due to the tip weight of the deployed samara blade; then the observed correlation between blade tip weight and body tilt angle is independent of whether or not the models had achieved steady state, equilibrium flight. Preliminary analysis suggests that a near one to one correlation between the tilt of the principal axis of rotation and body tilt is indeed the case. Therefore for the full weight model it would appear a higher bladetip weight would be required to achieve the desired body tilt angle.

Listed in Table 6.1-1 are the rotor speed ratios, λ ($\lambda = V/\omega R$, the ratio of rotor descent rate to rotor tip speed), for the tested samara configurations. These rotor speed ratios correspond to very high blade tip inflow angles (greater than 35 degrees) which, for the low blade tip incidence angles obtained experimentally, implies that the bladetip and therefore the entire blade operates at an angle of attack beyond blade stall. Also listed in this table are rotor alone drag coefficients (i.e. drag coefficients based on the rotor thrust minus the drag on the samara centerbody referenced to blade swept area). Overall the calculated drag coefficients are somewhat lower and have a greater spread than those obtained from Langley testing. The fact that they are in general lower is probably due to the fact that in most instances the models were still spinning up and had not reached steady state

flight conditions. Therefore the recorded velocities are probably higher than what they would be had steady state, autorotative flight been established. In addition the greatest experimental uncertainty is in the tunnel airspeed measurement as previously described in Chapter 5. The recorded airspeeds are probably higher due to this as well, in that the best indicator of test airspeed is at launch which usually involves a higher airspeed than that at steady state, equilibrium flight conditions since launch is at lower spin rates than the steady state values. Certainly, corroborating Langley test results, a rotor drag coefficient between .4 and .5 looks achievable with a stalled blade rotor. An even higher drag coefficient is possible if the samara blade could be flown unstalled, however, it is not obvious that this is readily doable at the rotor speed ratios of interest here.

Chapter 7: Conclusions and Recommendations

Section 7.1 Experimental Data

Many experimental difficulties were encountered during the free flight testing of IRAAM samara in the Wright-Patterson vertical wind tunnel. As a result most of the samara configurations flown never achieved steady state, equilibrium, autorotative flight. Two flights with full weight, 3.6 inch/5 inch height/diameter ratio IRAAM samara models came reasonably close to achieving steady state flight. The corresponding steady state sink rates and spin rates were near the design values of approximately 100 fps and 30 Hz; however, the body tilt angles were low. The low body tilt angles were the result of too low a blade tip weight. Rotor drag coefficients were slightly lower than the average value of 0.4 obtained in Langley spin tunnel testing. This is probably due to steady state flight not having been actually reached and poor quality airspeed data rather than to any inherent blade configuration differences. The relatively low rotor drag coefficients obtained are reflective of the fact that the blades tested were operating in a fully stalled condition. Otherwise the suspect nature of the flight conditions achieved and therefore the data measured do not warrant a more extensive quantitative data analysis. Most of these conclusions are of an observational, qualitative nature and relate more directly to the problem of obtaining quality terminal flight performance data for IRAAM samaras using free-flight model tests in the Wright-Patterson vertical wind tunnel.

Section 7.2 Wind Tunnel Facility

The major difficulty encountered is that of preventing the samara from flying laterally into the vertical net and sidewall of the test section and diffuser bell. Probably the most significant improvement one could make to the Wright-Patterson tunnel to make it more conducive to successful free-flight testing of samaras is to modify the velocity profile in order to keep the model near the center of the flow. The dish-shaped profile desired would be essentially flat in the center and increase continuously and fairly rapidly as one moves radially out from the center. This velocity profile modification could probably be accomplished using a combination of screens in the convergent section of the intake to the test section. It would involve a cut and try process with detailed velocity profile measurements to arrive at the right size, gauge, and placement of screens that produces the desired profile. The dish shape of the velocity profile in the Langley spin tunnel is believed to have been a major contributor to the successful free-flight samara testing conducted there.

An additional concern with regard to the tunnel velocity profile is the effect the vertical net has on it. The rake surveys that have been done to determine the profile were made without the net in place. The net may significantly retard the flow at its periphery creating a dome shaped rather than a dish shaped velocity profile. In particular the situation may be aggravated by the fact that, as a result of dyeing, the vertical net is smaller both circumferentially and lengthwise than intended. Rather than being

external to the tunnel flow, as designed, it may significantly interfere with it. Velocity profile measurements with the vertical net in place would permit better assessment of this possible interference. An experimental measurement of any existing radial flow component to the flow might also be useful in determining what might be done to improve free-flight testing in this facility.

As previously discussed, assuming one can keep the models away from the sidewalls and vertical netting, the next concern is having adequate control authority over the tunnel airspeed in order for the tunnel operator to be able to control the model's vertical position. It did appear that the operator had enough control authority to successfully "fly" at least some of the configurations tested. However, for other configurations and their transient flight characteristics it may be that the inherent lags between airspeed throttle input and response in tunnel airspeed cannot be overcome by any possible improvements in operator response as a result of flying such models. In this regard, the operator's control capabilities and the probability of successful flight could be improved by including within the operator's view the entire space within the diffuser bell. It is difficult to fly the model if you don't know precisely where it is or what its motion is. Possible solutions to the problem are to provide the tunnel operator with a video camera view of the interior of the diffuser bell or to provide for remote tunnel airspeed throttle control from within the test section chamber.

Section 7.3 Model Launch

The next problem to consider is that of improving the method of launching the samara models. At present the most successful method has been hand launching. This is principally due to the fact that the blade is already nearly fully deployed at launch. The difficulties associated with hand launching are repeatability, the number of successful launches per attempt, and that the spin rate at launch is relatively low. The latter may place significant adverse demands on the operator's control function depending on the transient flight characteristics of the model during spin up. In this regard the spin rates at which the Langley models were launched by hand were comparable to their steady state, equilibrium spin rates; which is not true for the Wright-Patterson samara configurations. Experience would probably improve the success rate of hand launching. In addition, other improvements, such as the suggested tailoring of the velocity profile, would probably improve the launch success rate as such stringent launch requirements, such as minimizing the lateral motion imparted to the model at launch, are relaxed.

Launching the model using a spin fixture offers the possibility of high launch repeatability as well as launching at spin rates closer to the steady state, autorotative spin rates. The difficulties associated with blade deployment subsequent to launch have already been addressed under experimental observations. Possibly modification of the samara blade design or packaging it in a particular way on top of the submunition can preclude some of these difficulties. For instance, one could try pre-twisting the blade opposite to the preferred twist direction to overcome the blade twist problem. A required

improvement to the spin fixture design is to provide for a means of ejecting the IRAAM samara model from the spin fixture. The obvious modification to the spin fixture design used is to include a pre-loaded spring ejection. Alternatively one would ideally like to launch the spinning samara model with the blade already deployed. The difficulty is that it adds considerable complexity to the spin fixture design in order to handle the load imbalances due to the high centrifugal loads at spin rate comparable to design steady state values. The design of such a spin fixture, that would handle a multiplicity of blade configurations and meet tunnel safety restrictions, is not readily apparent. But perhaps such a spin fixture design should be reconsidered.

Section 7.4 Samara Blade Configuration

Ideally in parametrically testing different samara blade configurations one would like to be able to isolate the effect of blade tip airfoil geometry from that of blade tip airfoil weight and chordwise c.g. position. In the present blade fabrication design the method of blade tip weight attachment by placement inside a pocket formed by a loop in the blade cloth material is simple, transmits the centrifugal loads on the tip weight to the blade material in an efficient manner, provides ready interchangeability of blade tip weights, and also satisfies safety considerations by providing complete enclosure of the tip weight. However, the shape of the blade tip pocket varies with the centrifugal and aerodynamic loading on the blade and in addition is irregular and not repeatable. It is recommended that in future

testing a blade fabrication design be chosen that allows for independent variation of blade tip airfoil/weight characteristics and still satisfies safety considerations. A blade tip airfoil/weight/blade attachment design that is capable of being full-specified and repeatable is required.

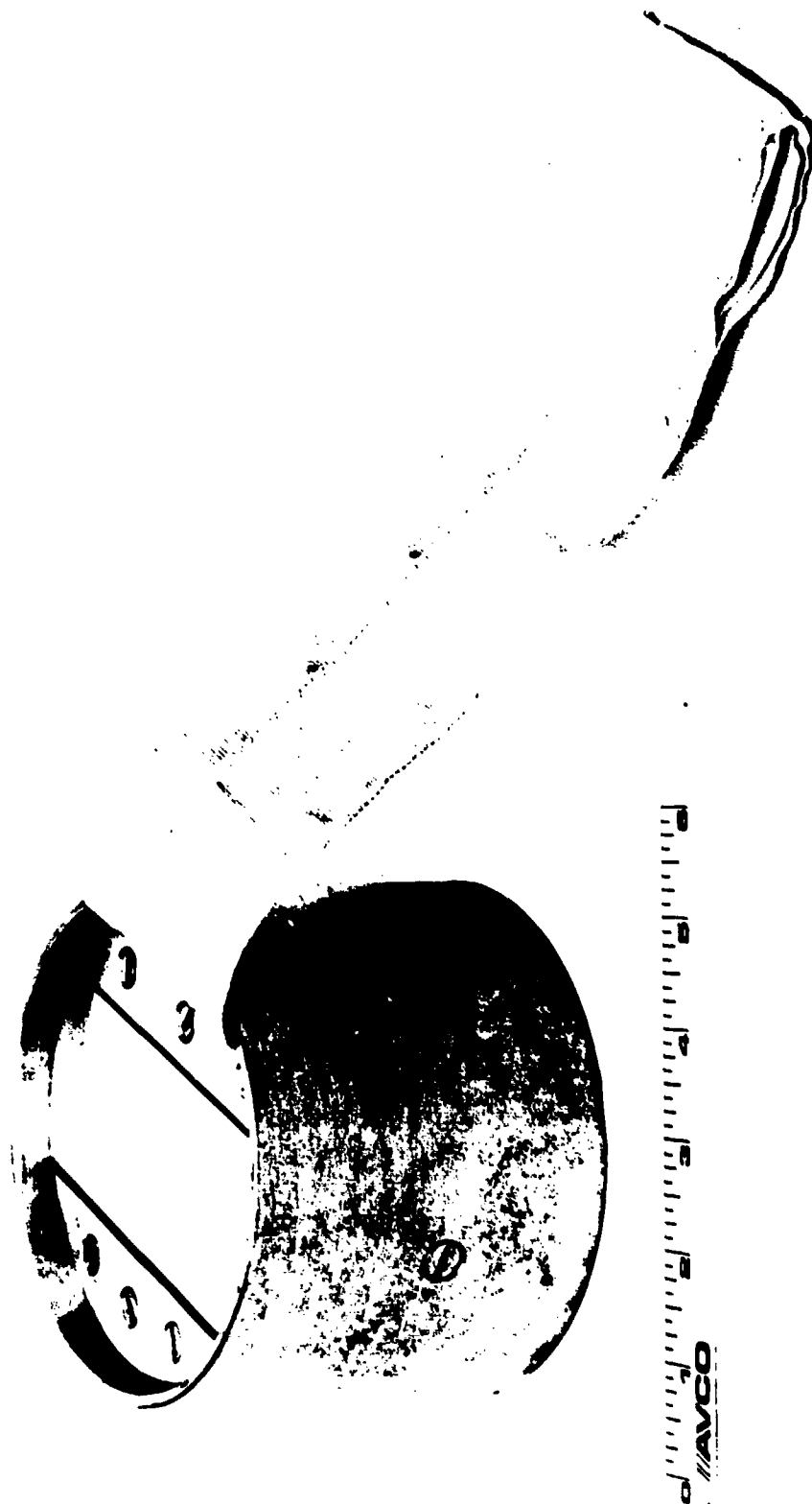
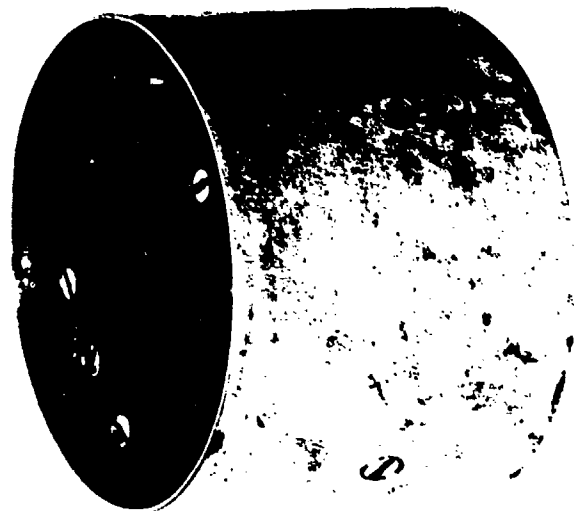
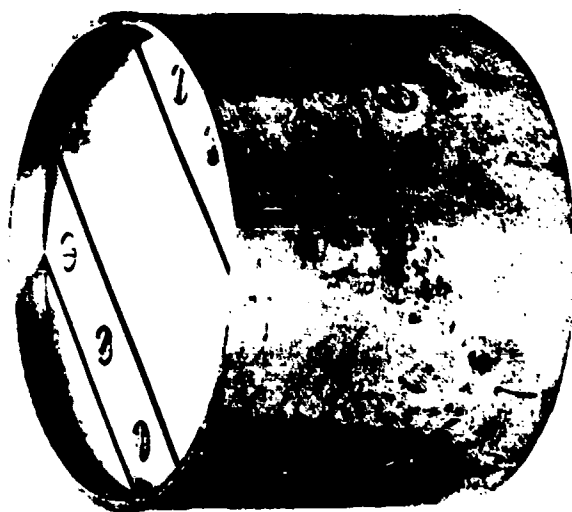
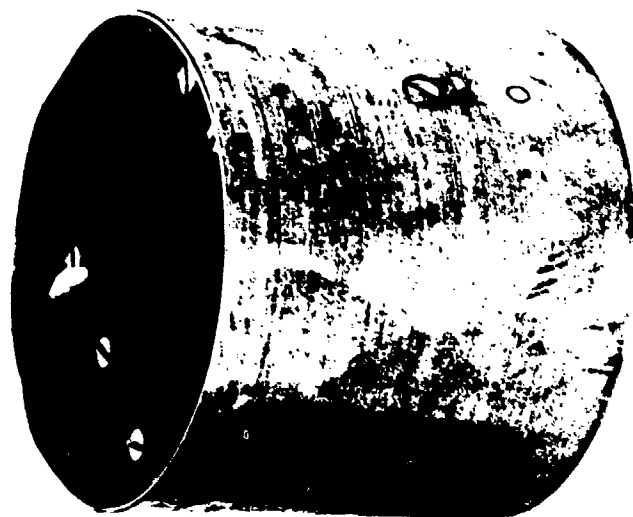


FIGURE 1.0-1 IRAAM Samara Model

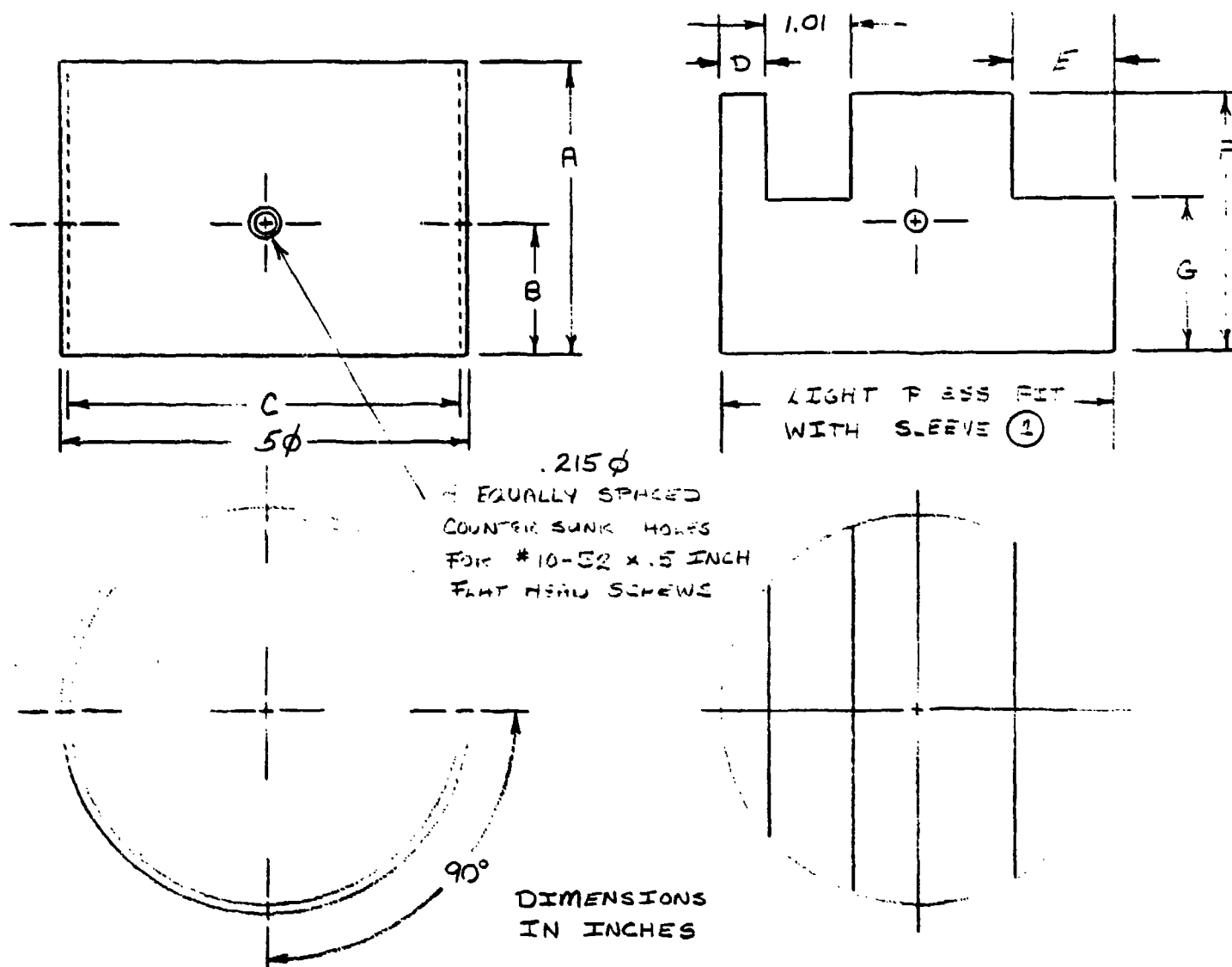


AVCO

FIGURE 2.1-1 Photograph of IRAAM Samara Centerbody Models

① STEEL SLEEVE

② CORE



CENTERBODY MODEL	1	2	3
CORE MATERIAL	LEXAN	AL	LEXAN
A	3.6	3.6	4.32
B	1.6	1.6	2.0
C	4.84	4.72	4.84
D	0.6	0.54	0.6
E	1.26	1.20	1.20
F	3.2	3.225	3.92
G	1.9	1.926	2.62

FIGURE 2.1-2 Schematic of IRAAM Samara Centerbody Model

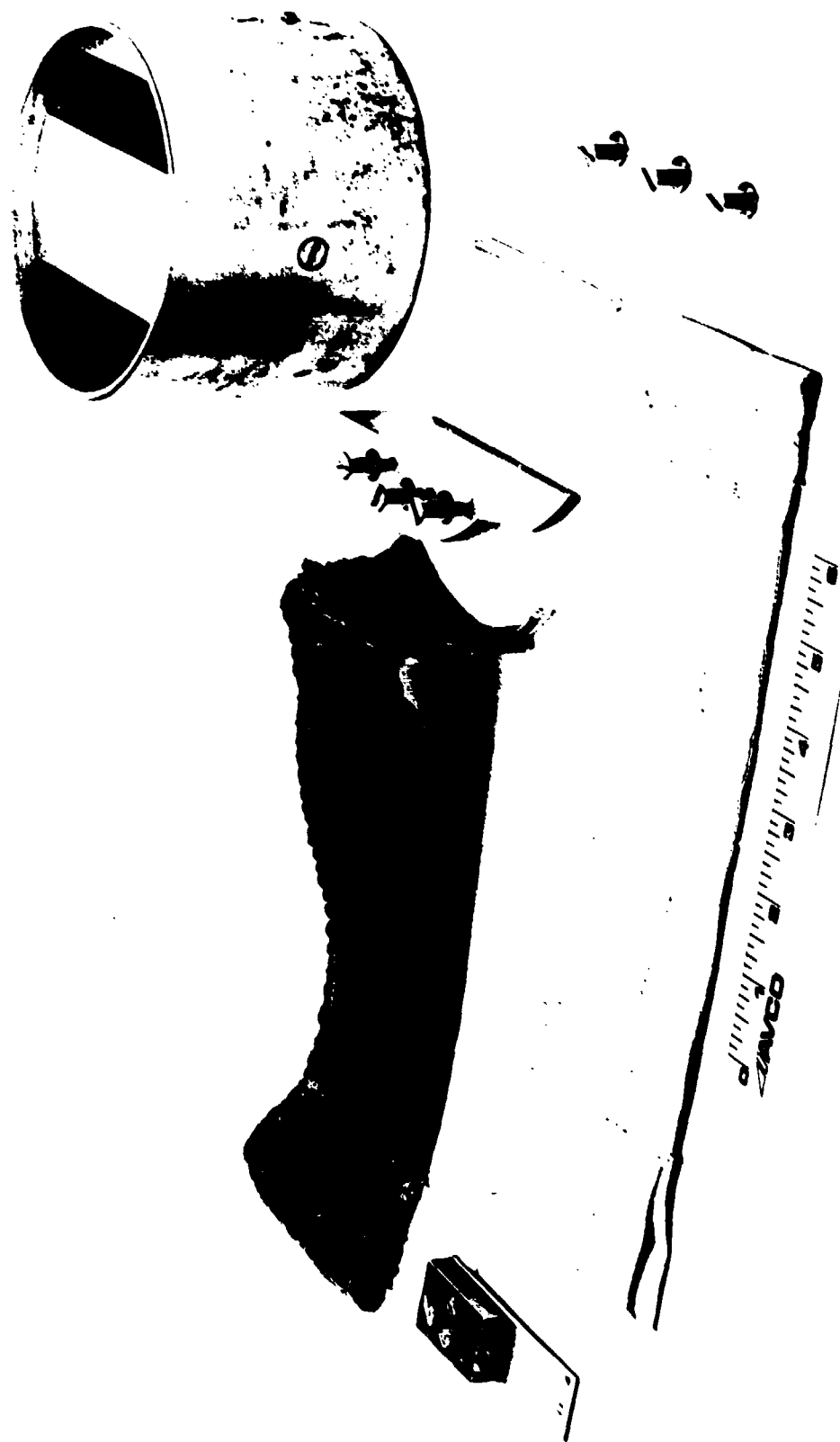


FIGURE 2.1-3 Photograph of IRAAM Samara Wind Tunnel Model Showing
Component Assembly

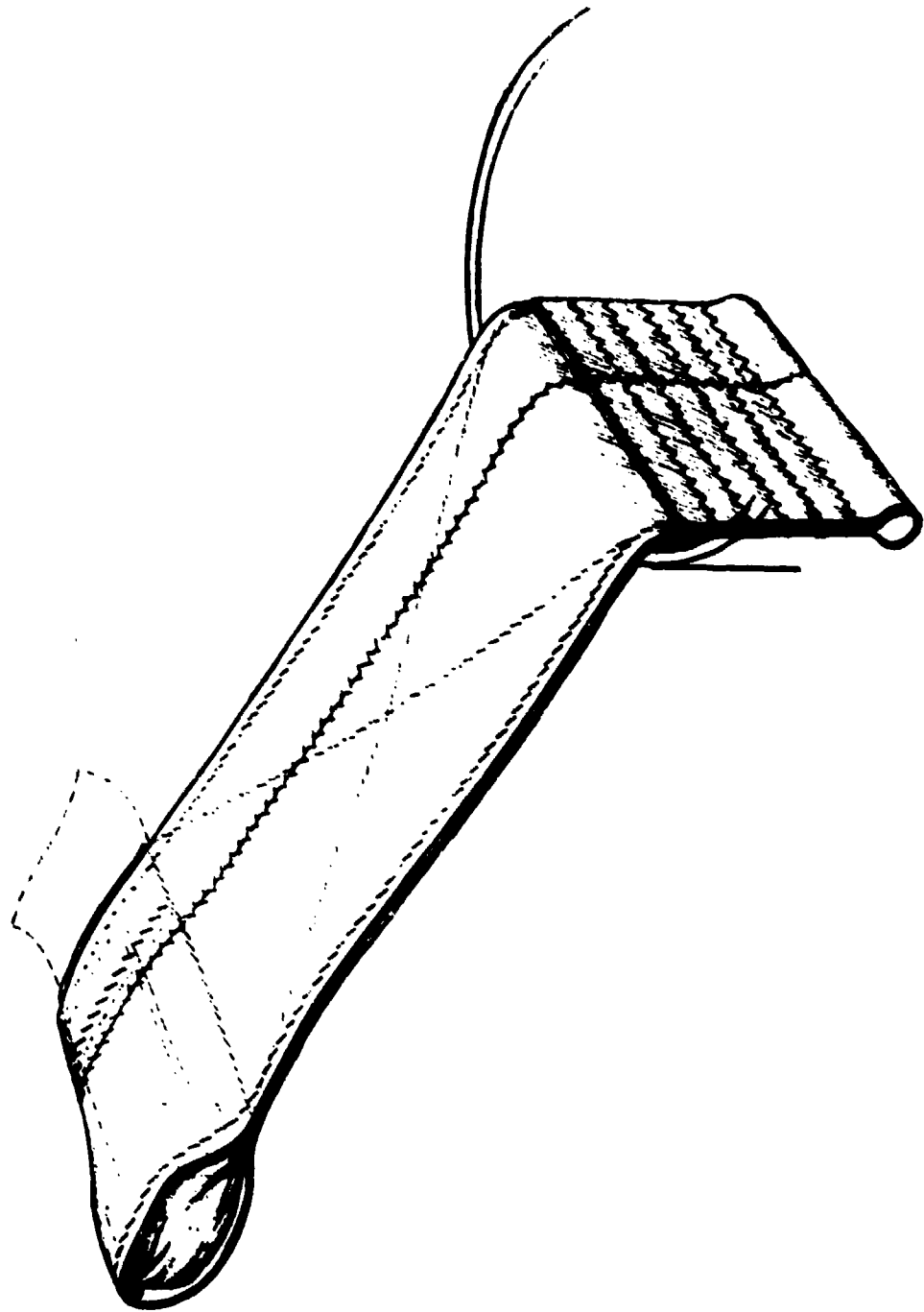


FIGURE 2.2-1 SCHEMATIC OF WEBBING TYPE BLADE CONSTRUCTION

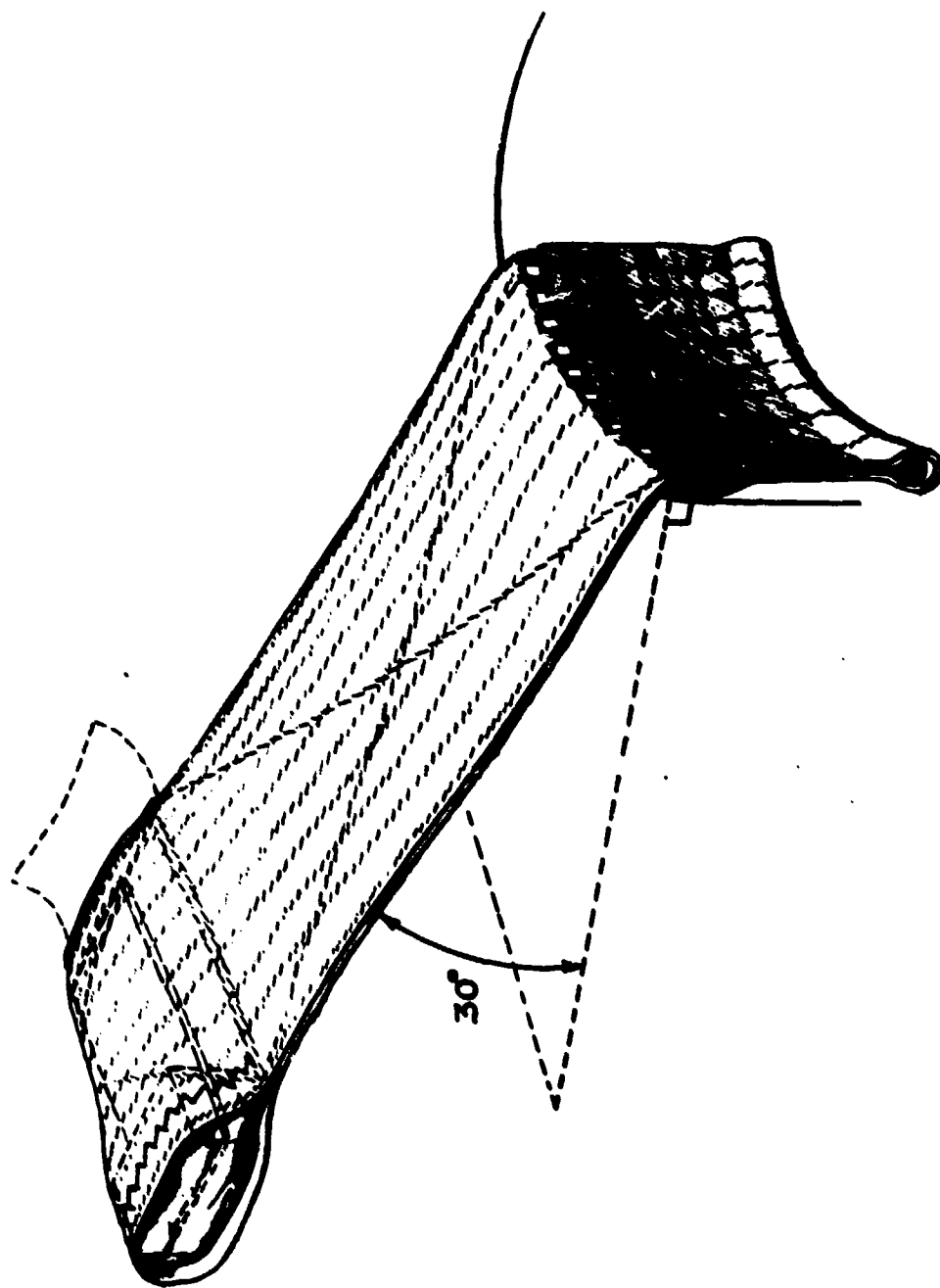


FIGURE 2.2-2 SCHEMATIC OF CORDED TYPE BLADE CONSTRUCTION

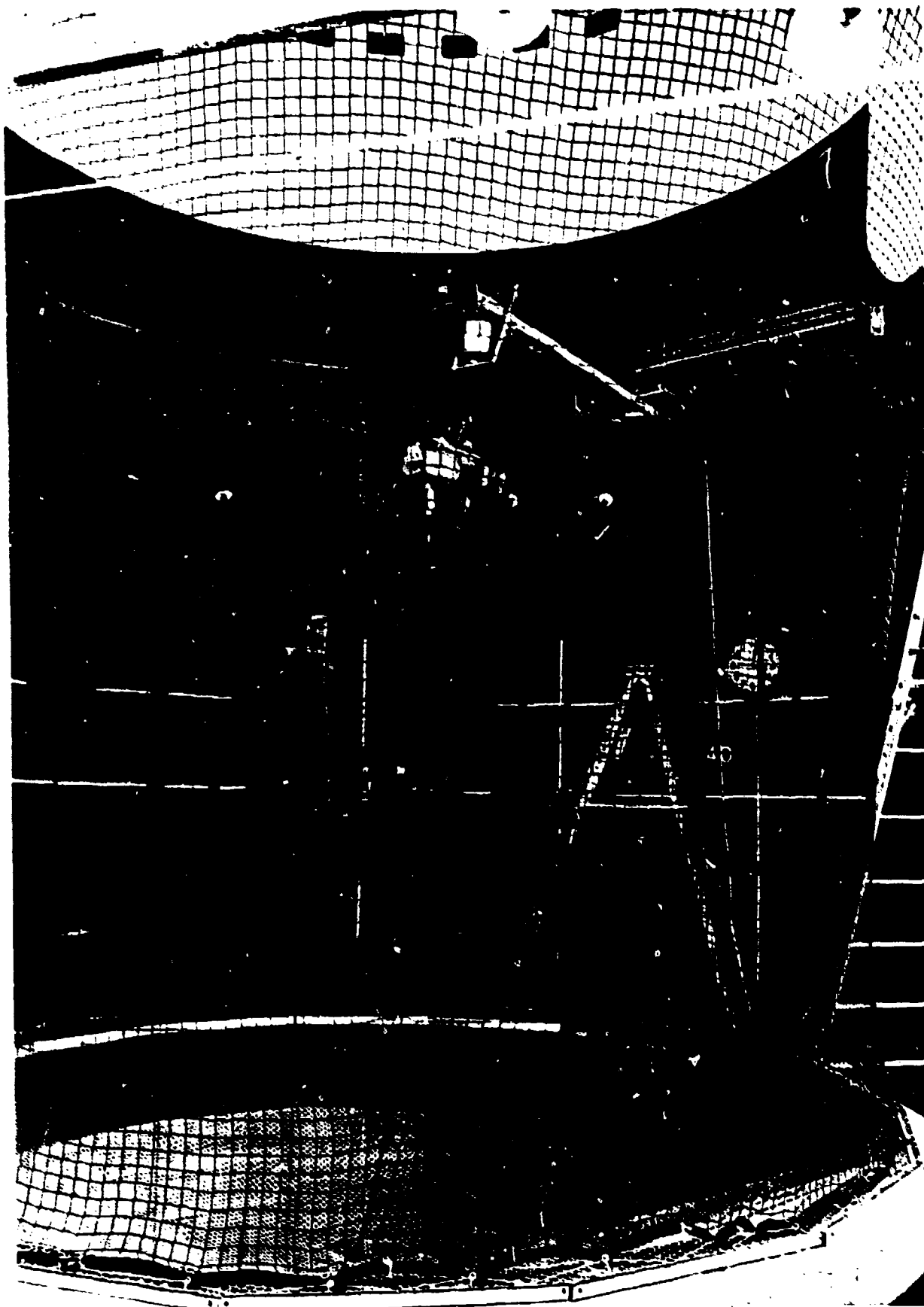


FIGURE 3.1-1 Photograph of Spin Fixture in Wright-Patterson Vertical
Wind Tunnel

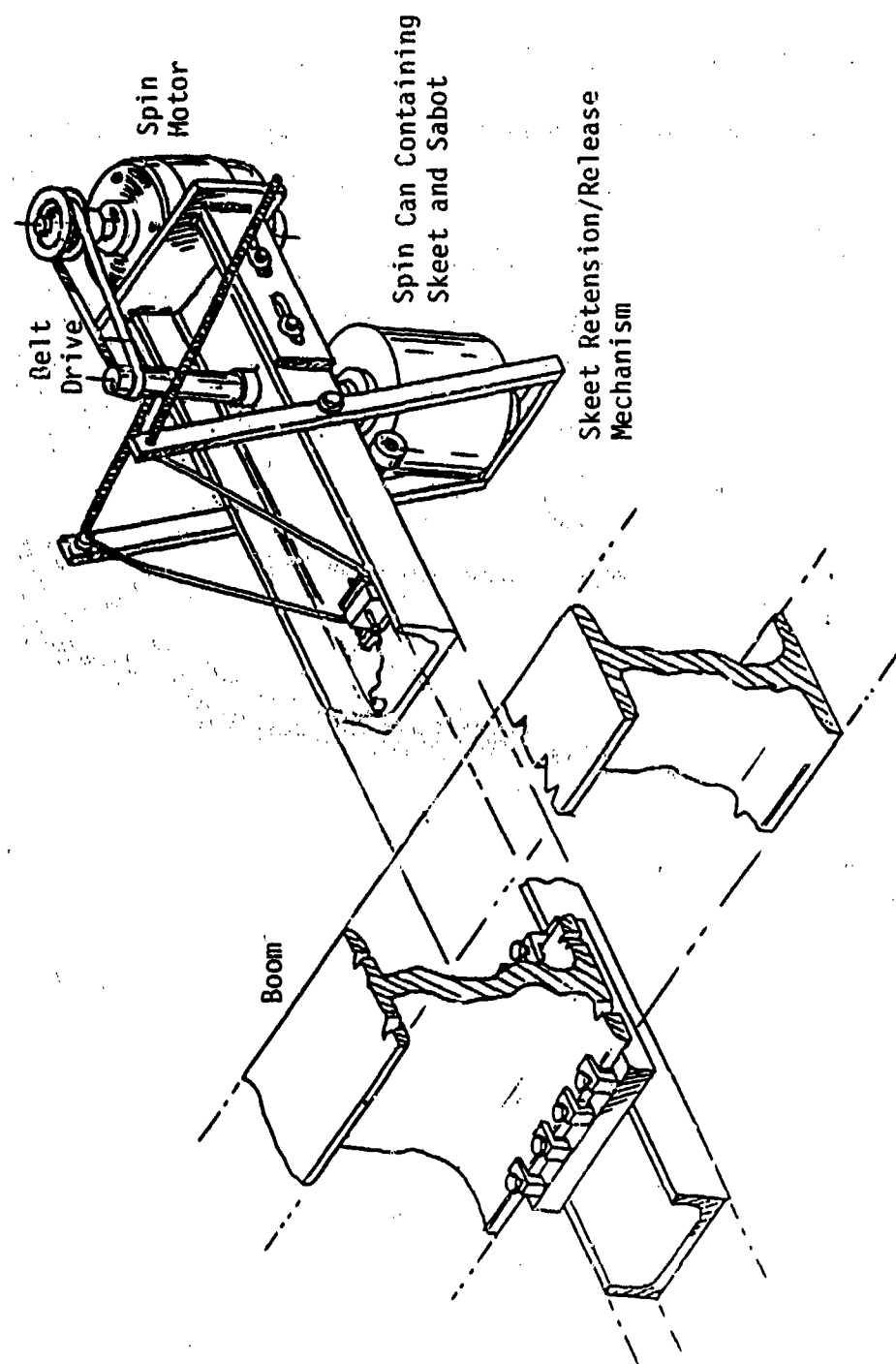


FIGURE 3.1-2a SCHEMATIC CRANE BOOM MOUNT

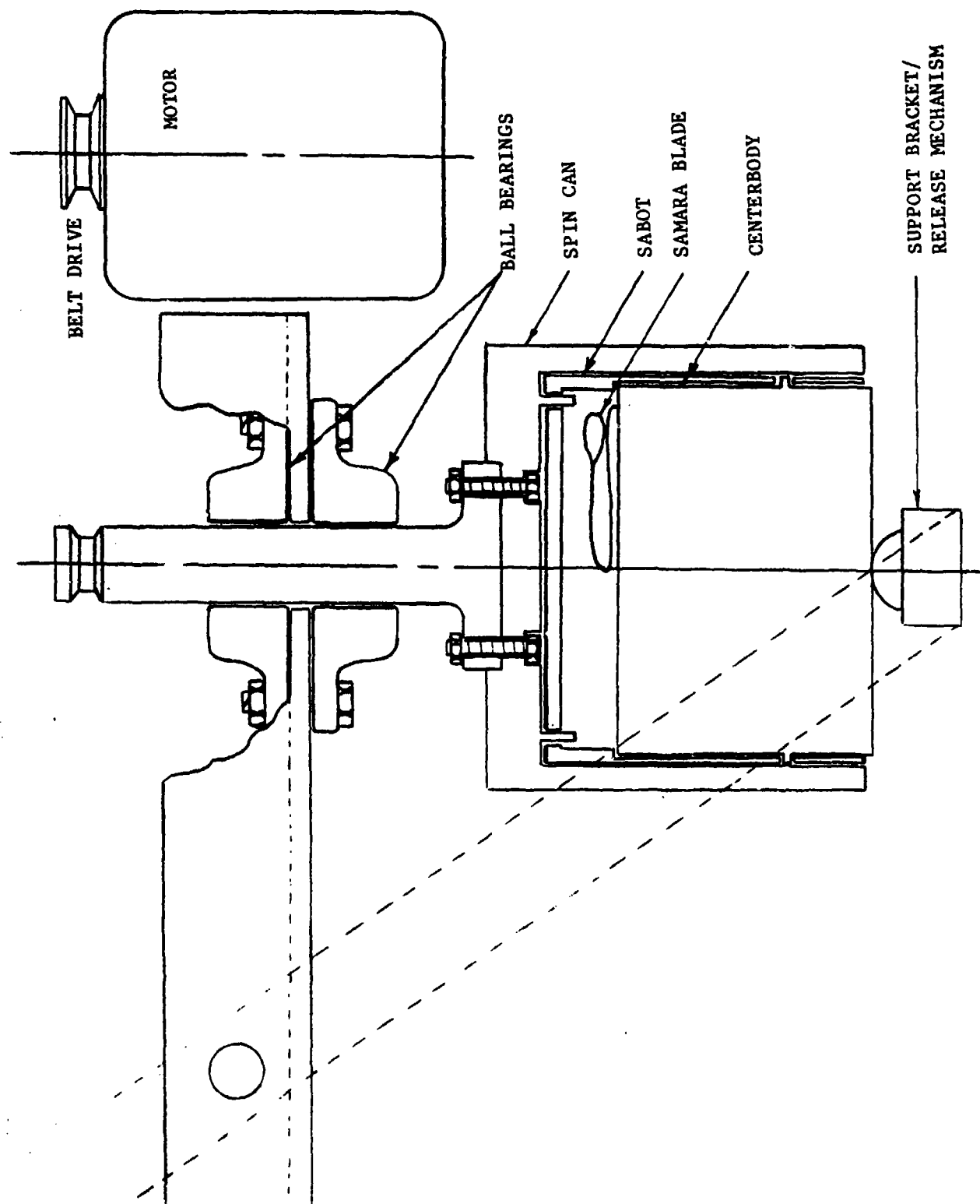


FIGURE 3.1-2b SCHEMATIC OF SPIN FIXTURE

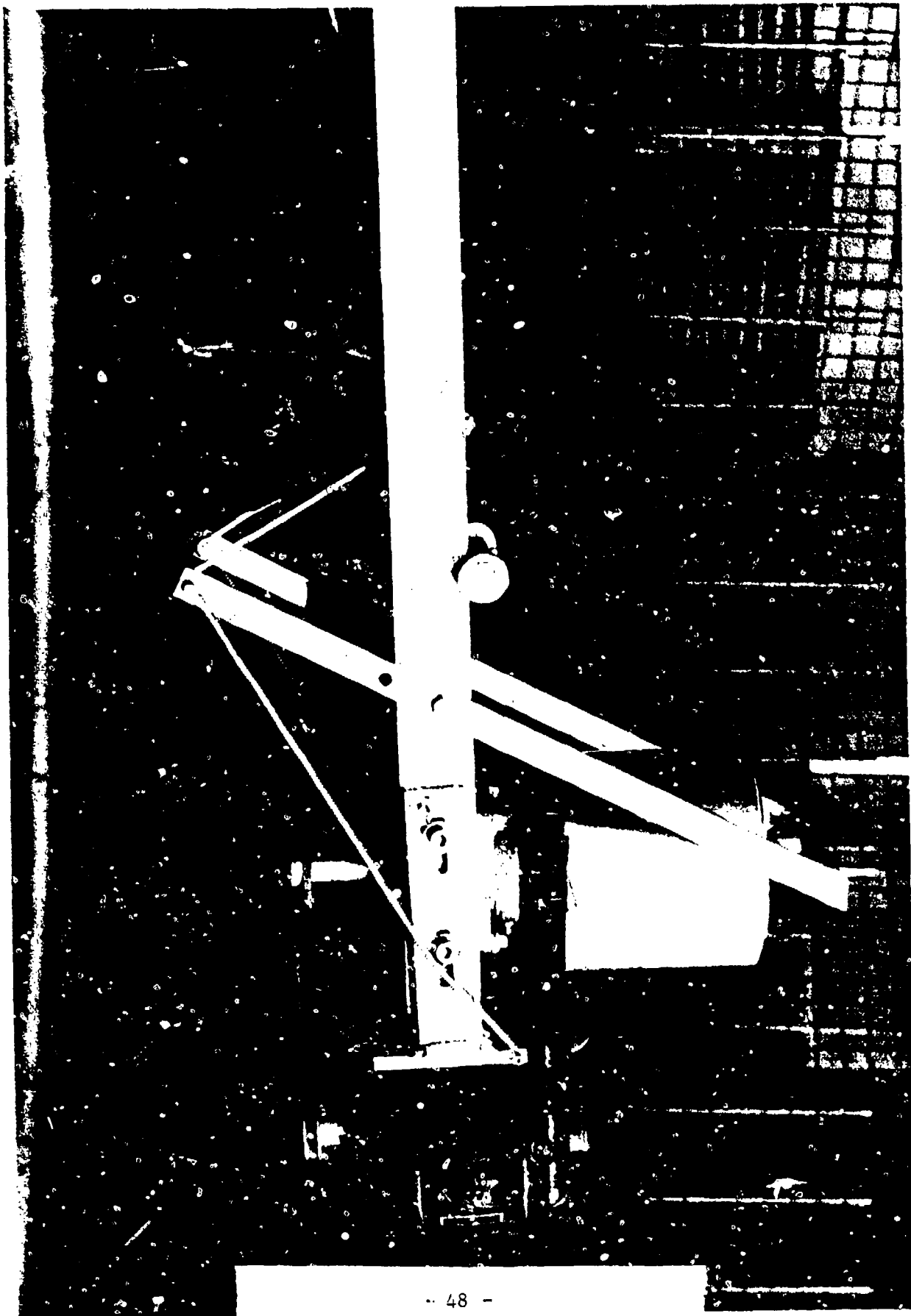


FIGURE 3.1-3 Photograph of Spin Fixture in Coiled Position with Saboted Model Inside

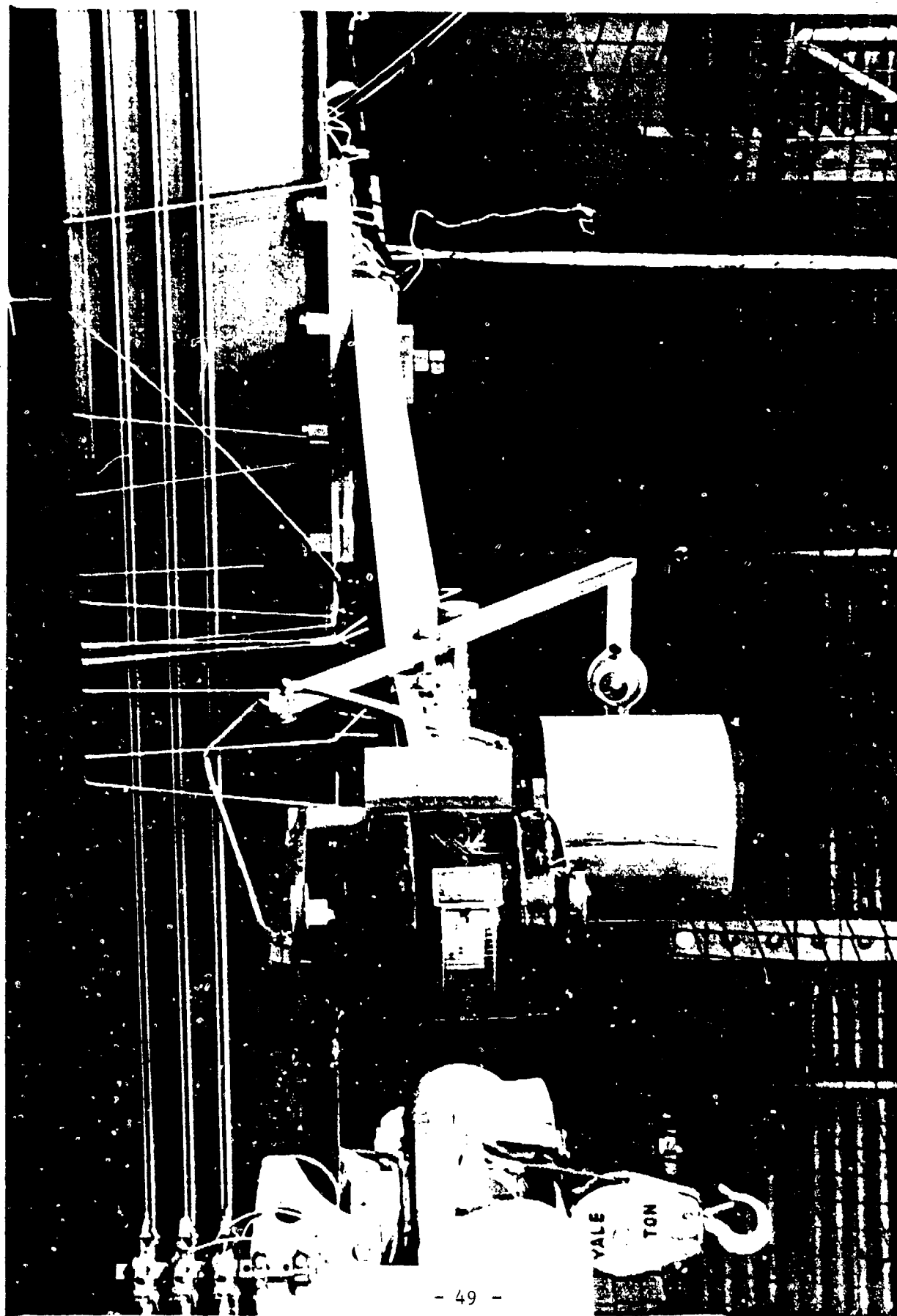
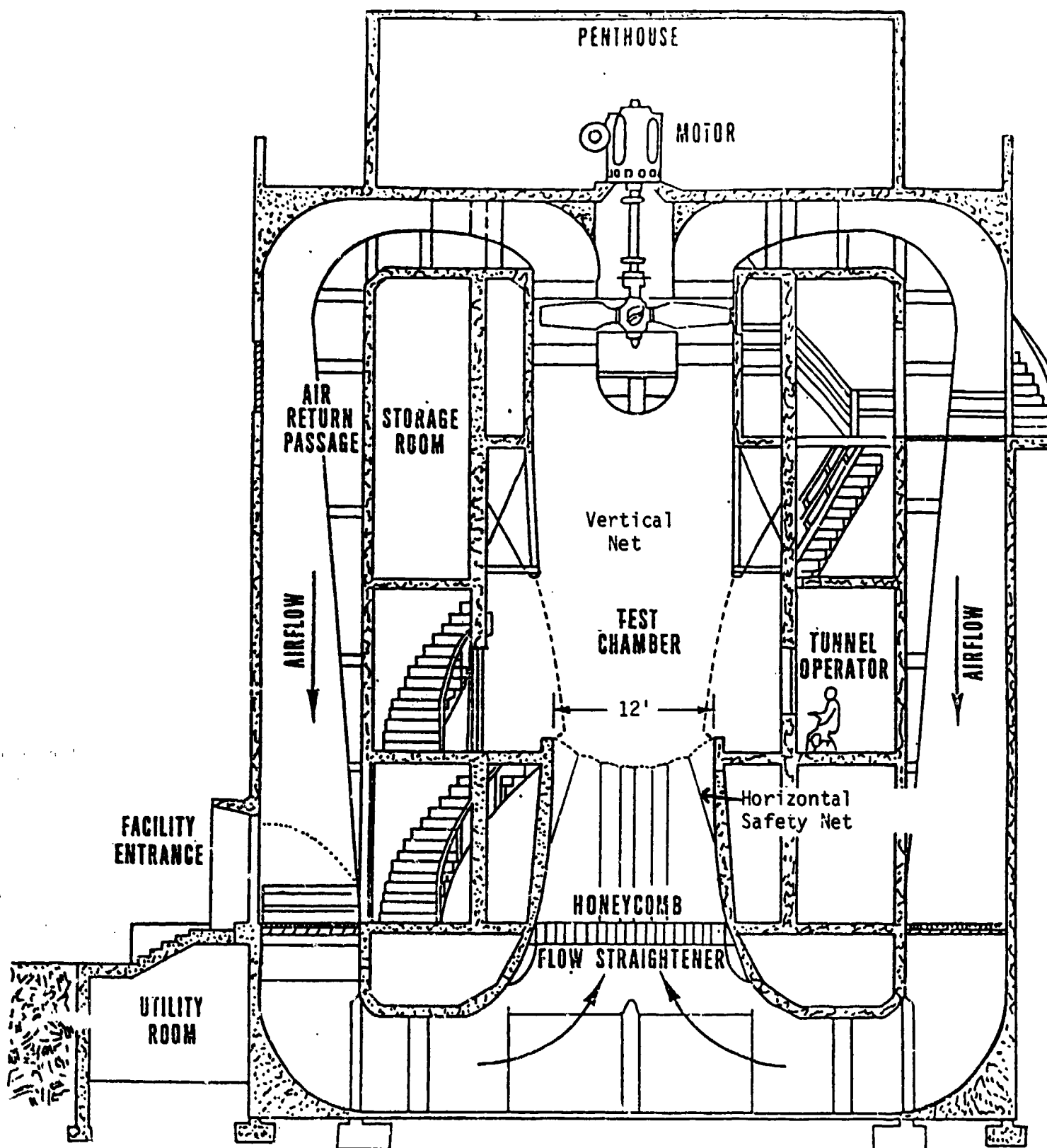


Figure 3.1-4 Photograph of Spin Fixture After Release of 100



VERTICAL WIND TUNNEL

WRIGHT-PATTERSON AIR FORCE BASE

FIGURE 3.2-1 Schematic of Wright-Patterson Vertical Wind Tunnel

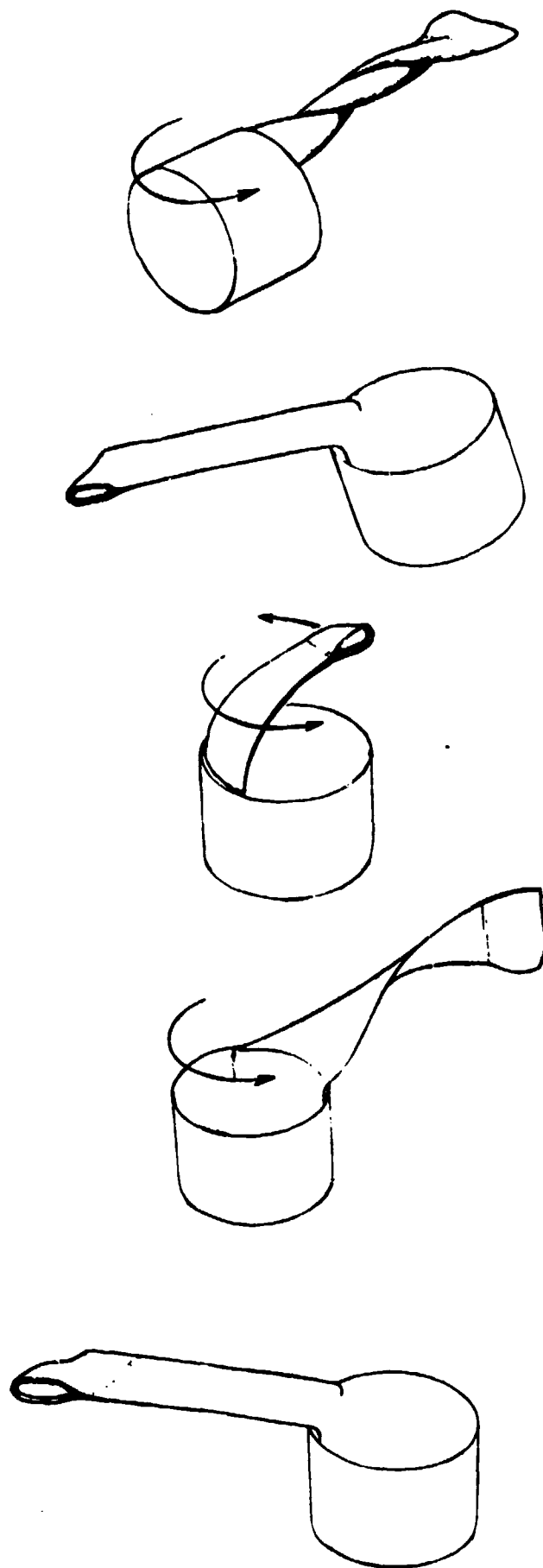


FIGURE 5.2-1 Sketch of Typical IRAAM Samara Flight Behavior Following Launch Using the Spin Fixture

TABLE 1.2-1

SAMARA BLADE PARAMETERS TESTED

LANGLEY SPIN TUNNEL - 1st Entry (December 1981)

- side mounted
- root location above base (% height): 0.24, 0.55, 0.76
- chord (cal): 0.6
- span (cal): 1.25, 1.85
- sweep (deg): 0, 20, 30
- root incidence (+ nose up) (deg): -20, -25, -30, -40, -50
- tip mass (% model mass): 5, 7
- tip mass c.g. (% chord): 25
- tip inverted camber radius (cal): 1, ∞
- fabric: nylon

LANGLEY SPIN TUNNEL - 2nd Entry (June 1982)

- top mounted
- root location in from O.D. (cal): 0, .1, .2, .3
- chord (cal): 0.6
- span (cal): 0.5, 0.75, 1.0, 1.5
- sweep (deg): 0
- root incidence (deg): 0, -10
- tip mass (% model mass): 2.5, 4, 5
- tip mass c.g. (% chord): 20, 25, 30, 50
- tip inverted camber radius (cal): 0.5, ∞
- fabric: nylon

Table 2.1-1

**IRAAM Samara Centerbody Geometry and Mass Properties
Wright-Patterson Vertical Wind Tunnel Tests of April 4-8, 1983**

Model	1	2	3
Height/Diameter (in/in)	3.6/5	3.6/5	4.32/5
Mass (lb_m)	3.78	7.69	4.63
C.G. Axial Location Above Base (percent height)	0.46	0.46	0.47
Axial Moment of Inertia, I_{xx} ($lb_m in^2$)	15.1	28.2	18.3
Transverse Moments of Inertia, $I_{yy} = I_{zz}$ ($lb_m in^2$)	11.1	21.3	15.5
Products of Inertia, I_{xy} I_{yz}, I_{xz} ($lb_m in^2$)	nominally zero		

TABLE 6.1-1 Test Data:

Wright-Patterson Vertical Wind Tunnel Testing of
ISAAH Samarap, April 4-8, 1983

Flight No.	Skeet Centerbody		Sawara Blades			Blade Tip Airfoil			Tunnel Data:			$\lambda^{-1} \frac{V}{\omega R}$	C_D of Rotor (referenced to blade swept area)	
	Height (in) (Dia = 5 in)	Weight (lbs)	Root Type	Blade Type	Root Location wrt Center (in)	Chord (in)	Span (in)	Weight (lbs)	C.S. Location (% chord)	Sink Rate (fps)	Spin Rate (rpm)			Body Tilt Angle (deg)
1	3.6	3.78	STR	WSE	1.77	3	7.5	0.027	0.188	110	860	15-21	1.56	0.08
2							5.0	0.022	1	95	1000	18	1.40	0.26
3									0.098	83	910	14	1.53	0.38
4							2.5	0.027	0.063	103	1110	10	1.36	0.12
5									0.188	107	750	13	3.22	0.53
6									0.078	115	870	5-15	3.51	0.58
7									0.063	114	1090	5-10	2.77	0.58
8					1.25				0.063	114	660	?	5.28	0.21
9						2	5.0	0.036	0.183	101	1260	19	1.26	0.20
10									0.092	93	1040	12	1.50	0.26
11									0.057	94	1500	8	1.05	0.25
12									0.195	96	540	40	1.64	0.21
13	14.22	1.63	STR	WSE	2.37	4	10.0	0.042	1	86	810	22-37	1.65	0.21
14							7.5	0.036	1	81	1090	26	1.15	0.27
15									0.105	103	1000	26	1.21	0.22
16							5.0	0.029	0.195	102	860	22-32	1.85	0.23
17									0.105	99	1070	12-13	1.44	0.25
18							2.5	0.025	0.069	114	870	20	3.47	0.22
19							7.5	0.028	0.195	95	920	28	1.15	0.15
20						3			0.188	97	1090	(-10)-(650)	1.57	0.16
21			STR	WSE	1.77		1	0.027	0.098	99	1600	18-20	1.07	0.30
22							5.0	0.022		93	1360	17-18	1.15	0.32
23										93	960	15-23	1.73	0.30
24										95	1200	12-20	3.54	0.34
25										90	1040	13-21	1.45	0.39
26										99	1410	19-21	0.61	0.17
27	3.6	1.69	STR	WSE	2.31	4	10.0	0.042	0.195	99	1720	15	0.14	0.27
28			1	WSE	1	1	7.5	0.036	0.165	103				